PROCEEDINGS, Twenty-Fourth Workshop on Geothermal Reservoir Engineering
Stanford University, Stanford, California, January 25-27, 1999
SGP-TR-162

CHARACTERISTICS OF MICROSEISMICITY IN THE DV11 INJECTION AREA, SOUTHEAST GEYSERS, CALIFORNIA

Ann Kirkpatrick, John E. Peterson, Jr., Ernest L. Majer, and Robert Nadeau
Lawrence Berkeley National Laboratory
One Cyclotron Road
Berkeley, CA 94720

ABSTRACT

Microearthquake (MEQ) occurrence surrounding the injection well DV11 in Unit 18 of the Southeast (SE) Geysers is investigated. Seismicity rates are compared to the injection rate, and to flow rates in nearby steam extraction wells, which were monitored during the Unit 18 Cooperative Injection Test in 1994 and 1995. The seismicity rate is seen to mirror both injection and production rates, although a time lag sometimes occurs. Waveform cross-correlation is performed for the MEQs in the DV11 area, and the events grouped into clusters based on waveform similarity. Relative location techniques applied to the events in two of these clusters show 7 events grouped into a volume of about 25 m in diameter, at an elevation of about -0.65 km msl and 5 events grouped into a vertically-oriented linear feature about 100 m in length, at about -1.8 km msl.

INTRODUCTION

It has been demonstrated by several investigators that microearthquake occurrence at the Geysers geothermal area is associated with both water injection and steam extraction (e.g., Eberhart-Phillips and Oppenheimer, 1984; Stark, 1992). However, the relevant changes in subsurface conditions caused by these activities, and the mechanisms by which these changes cause MEQs remain unknown. If more were understood about the relationships between these processes, then MEQ occurrence and characteristics could possibly serve as indicators of reservoir conditions, and thus be used as a reservoir management tool.

In order to collect data to address these questions, Lawrence Berkeley National Laboratory (LBNL) installed a network of digital seismometers at the SE Geysers in 1993. This network, and results of several studies utilizing data obtained from the network, have been described in previous reports (Kirkpatrick et. al., 1995, 1996, 1997). In addition, Unocal operates a network of analog seismometers over a larger area of the Geysers, and provides a catalog of MEQs hypocenters in the SE Geysers to LBNL. The locations of both networks are shown in Figure 1. While the LBNL network is capable of locating events more accurately than the Unocal network, and can be used for more sophisticated source mechanism analysis, the Unocal network has operated for a long period of time with great reliability and is thus invaluable for studies of MEQ rate variations over time.

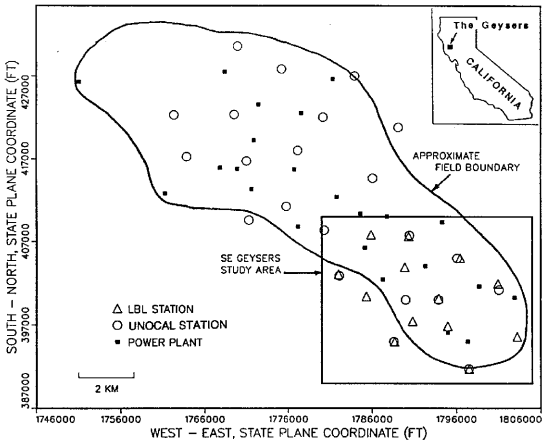

Figure 1. MEQ monitoring networks at The Geysers. The SE Geysers study area is shown in detail in Figure 2.

The Unit 18 Cooperative Injection Project was a cooperative program between Unocal Corp., PG&E., Northern California Power Agency (NCPA), Calpine Corp., and the U.S. Dept. of Energy whose purpose was to monitor and define the reservoir response to water injection into steam-production intervals at The Geysers. Well DV-11 in Unit 18 of the Unocal lease was chosen as the injector for this project, due partly to its proximity to producing wells in the Unocal, NCPA, and Calpine lease areas. Injection began in late December 1993, and continued through January 1995. During this time, flow rates, well-head pressures, and well-head temperatures were monitored daily in the surrounding wells, and were

made publicly-available. Also made available were the 3-D well courses, and steam entry and top of felsite information. After the end of the Unit 18 project, injection into DV11 was intermittent until the start-up of the SE Geysers Effluent Pipeline project in September 1997. At that time, treated sewage effluent from the Lake County began to be piped to the SE Geysers, and has provided a steady source of injectate into DV11 as well as other Unocal, Calpine, and NCPA injection wells.

The LBNL MEQ network was in operation from January 1994 through October 1995, and has operated from August 1997 through the present time. The Unocal network has been continuously in operation since 1988. The existence of the unique data bases provided by both these networks, in combination with the DV11 injection history and the information made public as part of the Unit 18 Cooperative Injection Project, provides a unique opportunity to investigate the seismic response of a steam-producing geothermal reservoir area to the introduction of large amounts of cold injectate fluids.

SPATIAL SEISMICITY PATTERNS

The general pattern of seismicity over the entire SE Geysers study area is shown in Figure 2. Shown are MEQ hypocenters detected by the LBNL array for a 3-month time period in 1998. This general pattern has been noted in the data from 1994-1995, and has been discussed in previous work (Kirkpatrick et. al., 1996). The events occur in both clusters and in more diffuse patterns. Some of the clusters surround injection wells, while others surround particular steam extraction wells. Not all injection wells have associated seismicity, nor do all areas of steam extraction. The depths of almost all of the events range from about the top of the producing reservoir to at least the total depths of the deepest wells.

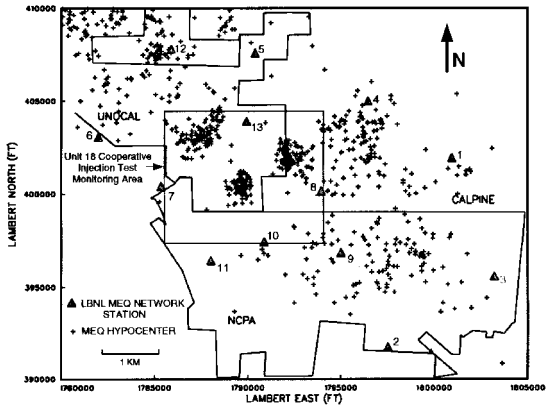

Figure 2. MEQ hypocenters detected by the LBNL MEQ Network in the SE Geysers study area, for the time period 7/1/98 to 9/30/98. The Unit 18 Cooperative Injection Test Monitoring Area is shown in detail in Figure 3.

Figure 3 shows MEQ hypocenters located in the DV11 area from January 1994 to October 1995. The well traces for the injector DV11 and the surrounding production wells are also shown.

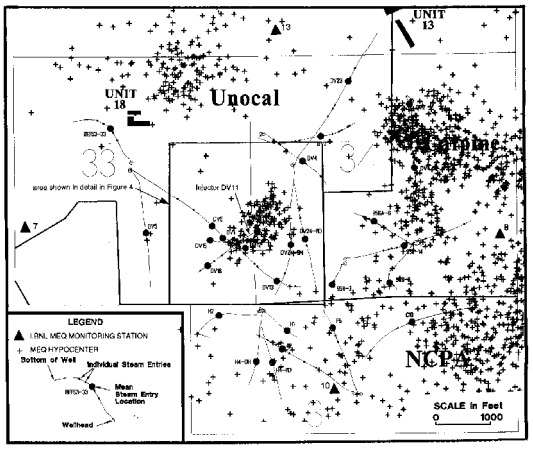

Figure 3. MEQ hypocenters in the Unit 18 Cooperative Injection Test Monitoring Area during and after the injection test (January 1994 to October 1995), and the locations of the wells monitored. The cloud of seismicity immediately surrounding the injector DV11 is shown in detail in Figure 4.

The cloud of events immediately surrounding DV11 is shown in both plan and depth section in Figure 4. The locations are slightly different from those shown in Figure 3 because the data for these events was filtered to remove 60 Hz noise, the arrival times re-picked and then the events relocated. The cloud of 149 MEQs extends to the west of the injection well, but not to the east, in both the north and south directions. Interestingly, the wells to the west and south of DV11, in both the Unocal and Calpine lease areas, showed the greatest increases in flow rate due to the injection (Voge et. al., 1994) The DV wells to the east and northeast showed less response to the injection, and the Calpine wells did not appear to respond at all.

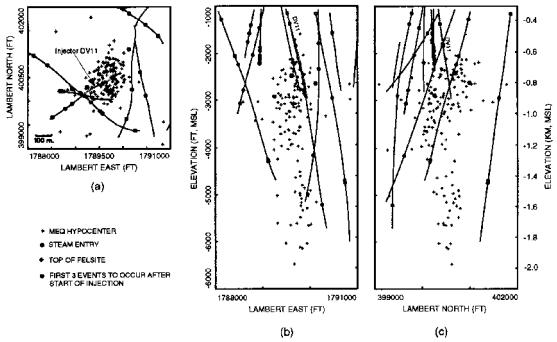

Figure 4. MEQ hypocenters in the DV11 injection area, January 1994 to October 1995. The locations

differ slightly from those shown in Figure 3 because the data were filtered, the arrival times re-picked, and the events re-located. (a) plan view, (b) east-west cross-section, (c) south-north cross-section.

The cloud of events extends in a tube downwards. While the lateral dimensions of the cloud is about 300 m, the vertical dimension is four times the horizontal, about 1200 m. The tube is centered below the one steam entry in DV11; the top of the cloud is about 300 m below that steam entry. The bottom 300 m of the DV11 well bore extends into the top of the event cloud. Some of the deepest events occur below the total depth of the deepest producers in the vicinity. The events occur mainly in the felsite, with virtually none in the unit above the felsite contact. Steam entries, in contrast, occur in the wells in both the felsite and the overlying unit.

The error in the LBL event locations is estimated to be up to 100 m, due to arrival time estimation errors and to errors in the velocity model used to locate the events. For this reason, it is difficult to discern structure within the cloud of events. Waveform cross correlation techniques that have the potential to reduce these errors were applied to the LBNL seismic data in this area. These results are described in a later section.

TEMPORAL SEISMICITY PATTERNS

The injection rates for DV11 are graphed in Figure 5. The total volume injected for each month is plotted; daily flow rates reported ranged up to 848 gpm during the Unit 18 Cooperative Injection Test. Injection began in late December 1993; prior to that time DV11 was a producing well. Injection for the test ceased in February 1995; from that date to late September 1997 water was injected into DV11 only intermittently. In October 1997 DV11 began to accept injectate from the SE Geysers Effluent Pipeline, and in December 1997 injection rates reached a steady level which continue through 1998. The combined production rate for the DV wells in the Unocal lease area, provided during the Unit 18 Cooperative Injection Test, is also shown in Figure 5. Immediate increases in production followed injection, and decreases in injection were followed by decreases in flow rates.

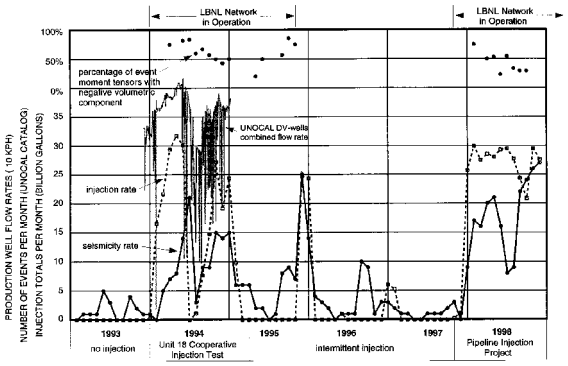

Figure 5. Injection rate into DV11 and seismicity rate in the surrounding area for January 1993 through November 1998. The flow rate for all the Unocal DV-wells combined is shown for the Unit 18 Cooperative Injection Test period. The circles at the top of the plot represent the percentage of events for each month, whose moment tensors had a negative volumetric component. By definition, the remaining percentage had a positive volumetric component.

Seismicity rates, in number of events per month, for the DV11 area are also plotted on the graph in Figure 5. Data from the Unocal catalog is only used because of the completeness of its record, compared to the periodic nature of the LBNL network. In 1993, prior to the start of injection, seismicity in the area occurred at a rate of zero to five events per month. The number of events per month began to increase in February and March 1994, two to three months after injection began. This is in contrast to the production increases which were seen immediately. The peak seismicity rate was reached one month after peak injection and production rates were reached. A sharp decrease in seismicity then closely followed the sharp decrease in injection rate June-July 1995, with a lag time of about one month. The next sharp increase in injection rate was again followed by a sharp increase in seismicity rate, this time with no lag. The seismicity rate also fell simultaneously with the cessation of injection at the end of the Unit 18 Cooperative Injection Test.

During the period of intermittent injection (1995-1997), a two-month period of high injection rate coincided with a sharp increase in the seismicity rate. The seismicity rate did not change, however, during another two-month period of increased, but only moderately high injection rate. There were also two periods of increased seismicity that were not associated with any increase in the injection rate.

An increase in seismicity is also observed starting in December 1997, simultaneously with the increase in injection due to the SE Geysers Effluent Pipeline

Project. The overall seismicity rate remained high in 1998 at the same time as the injection rate remained high; however, there were fluctuations in seismicity rate that were not reflected in variations in the injection rate. In addition, the overall trend of the seismicity rate increased in 1998 while the injection rate was fairly constant.

Locations of the events detected by the LBNL network in the DV11 area for the first six months of injection in 1994 were looked at in detail, in order to determine if the first events to occur after injection began were located near to the injection well, with later events migrating out away from it. This, however, appears to be the case in only a very general sense, in that the events located below -1.2 km msl did not occur until late May 1994, several months after the seismicity above -1.2 km msl began. The first three events detected after injection began (detected in February 1994) are highlighted from the rest of the seismicity in Figure 4. These three earliest events are widely spaced, up to 150 m apart and are located up to 200 m away from the injection well bore. Because the magnitudes of errors in the routine locations of events detected by the LBNL network are almost on the order of these differences in location, however, it is difficult to interpret relationships between these three events and the injection well, or between most of the events in the entire cloud. In an effort to begin to be able to study such individual events in more detail, and to identify related events and discern their relationships to each other and to conditions within the reservoir volume subjected to injection and extraction we applied waveform similarity analysis to the data in the DV11 area. In addition to providing a basis for the grouping of events, the techniques have the potential to greatly increase the accuracy of both relative and absolute event hypocentral locations.

WAVEFORM CROSS-CORRELATION ANALYSIS

We used the waveform cross-correlation techniques developed by Nadeau et. al.(1995), which they applied to MEQs detected by a network installed at Parkfield on the San Andreas fault, similar to the SE Geysers MEQ network. The waveform recorded at a particular station for one event is compared with the waveforms recorded at that same station for every other event. A cross-correlation coefficient, Xc, is obtained for each comparison. For identical waveforms, Xc=1, while Xc=0 indicates no similarity between the waveforms. This is repeated for every other station recording a waveform for this event; then this entire process is repeated for every event. The end result is a measure of similarity between pairs of events based on the similarity of their waveforms. The utility of this method is based on the principle that two events occurring in the same place with the same mechanism (i.e., orientation and direction of displacement at the earthquake source) will produce the same pattern of radiated energy, and thus an identical recorded waveform at each common station (assuming the properties of the path have not changed between the time of the two events). Small variations in location or mechanism between two events will produce small differences in waveforms, while larger differences in location or mechanism produce more different waveforms and consequently lower values of Xc. Thus two events can occur in the same place, but if they have different mechanisms they will not have a high Xc. Likewise, events that are separated by some distance (up to a certain limit) can have high Xc if they have a similar mechanism.

Applying this procedure to the 149 events located in the DV11 area in the 1994-1995 time period resulted in the identification of several groups of events that have similar waveforms, that we will term "clusters." Any number of criteria can be used to define what is "similar." For example, the criteria that two events are "similar" if the waveforms at five or more stations that they have in common have Xc's of 0.800 or above, resulted in the grouping of 26% of the events into 12 different clusters consisting of between 2 and 10 events each. At the Xc=0.750 level, 52% of the events group into 11 clusters with 2 to 48 events in each cluster. As the criteria are changed, some clusters merge while new clusters are also formed. Only 10% of the events group into clusters at the Xc=0.850 level.

Two of the clusters identified using the Xc=0.800 criteria were studied in detail. The hypocenters of these events are shown in Figure 6. Each event in each cluster is identified by the Julian day on which it occurred. The 7 events in the shallow cluster (located at about -0.7 km msl) occurred over a time period of 88 days, from Julian day 077 to 165 in 1994, and the 7 events in the deep cluster (located at -1.5 to -1.9 km msl) occurred over a time period of 69 days, from 098 to 167 in 1997. The waveforms recorded on the vertical component of Station 8 for each event in both clusters is shown in Figure 7. Visually, the waveforms within each cluster are very similar, while they are very different between the clusters.

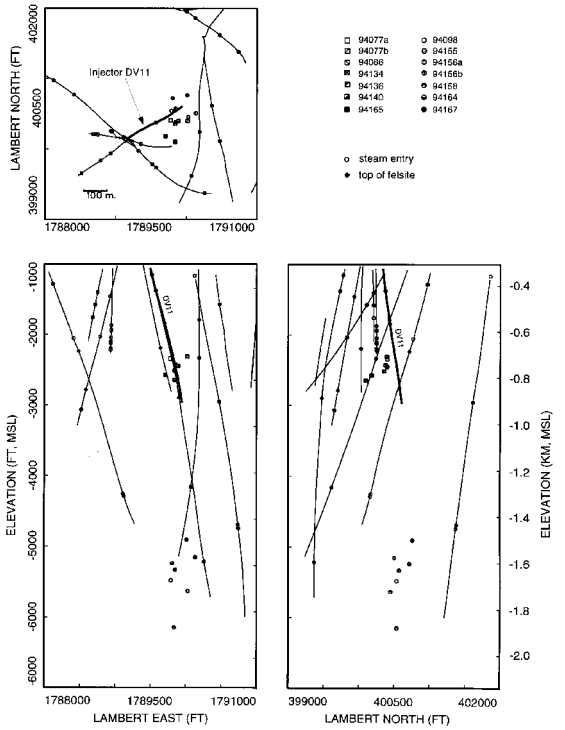

Figure 6. Hypocentral locations for the two clusters identified in the DV11 area that are discussed in the text. The arrival time picks determined using first break are used in the location routine.

The locations shown in Figure 6 were obtained using the routine location algorithm, and used the best estimated arrival time picks obtained from visual identification of the first break of the P- and S- wave phases. Arrival time picks can be in error up to 5 samples (0.01 sec) due to low signal-to-noise ratio, or an emergent arrival. If the estimated error in arrival time pick is greater than 5 samples, the arrival time is generally not picked and that information cannot be used in locating the event. Because the P- and S-wave seismic velocity model that is also used in the location algorithm does not perfectly reflect reality, the more stations that are used in the event location, the more the errors in the velocity model will average out and the greater the confidence in the event location. Because of these issues, the errors in the locations of each event in the shallow cluster is about on the order of the dimensions of the cluster, so that detailed conclusions regarding the spatial-temporal distribution of the events within the cluster cannot be made. For the deep cluster, the location error bars are probably somewhat smaller than the vertical dimensions of the cluster so there is more confidence in the vertical relationships between the events.

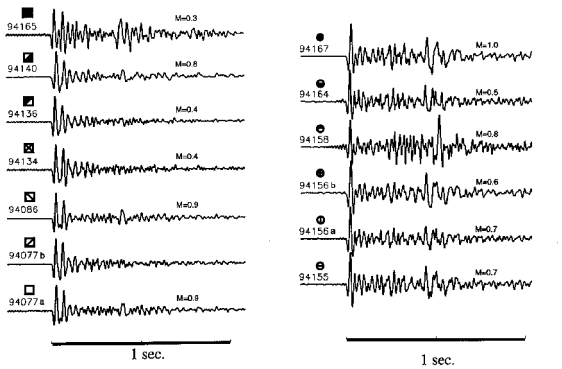

Figure 7. Waveforms for the vertical component of LBNL Station 8, for two of the clusters identified in the DV11 well area. The hypocentral locations of the events, identified by Julian day, are shown in Figures 6 and 8. Magnitudes are also given.

To address these location error problems, we performed additional cross-correlation analysis on the events in each cluster. The aim is to improve the accuracy of the arrival time picks, and to add arrival time picks at stations that lack them due to noise obscuring the first break, if possible. For each group of waveforms, consisting of the waveforms recorded at the same station for all events within a cluster, a reference pick is chosen at the waveform exhibiting the clearest first break. The other waveforms from that station are then aligned with that waveform at the point where the Xc value is maximum, and the arrival time for the new waveform is picked to align with the pick from the reference station. In effect, the arrival time is now being estimated based on the character of the energy contained in the wave pulse, which is not as affected by the noise which often obscures the first break.

In this way, new sets of arrival times were determined for all the events in the two clusters, and the events relocated. The number of iterations used in the procedure to find the minimum travel-time residuals were allowed to increase; otherwise all parameters remained the same. The event relocations are shown in Figure 8. It is immediately apparent that the events cluster more tightly. The distance between events in each cluster has been significantly reduced so that the events in the shallow cluster define a volume of 25 m across, and the deep events define a vertically-oriented linear feature about 100 m long, although both clusters contain one event separate from the main cluster. Also, one of the events from the deep cluster was not included in the relocation because it lacked arrival times. In contrast, the routine event locations defined a shallow cluster of dimension about 100 m, and the depth range of the deep cluster events was about 200 m. A consistent station set was used for

each cluster; therefore all errors in the velocity model average out for each event in the cluster in the same way, making the relative location between events in each cluster highly reliable. The absolute locations of the clusters have also changed somewhat, and become more accurate, we believe, due mainly to the additional iterations.

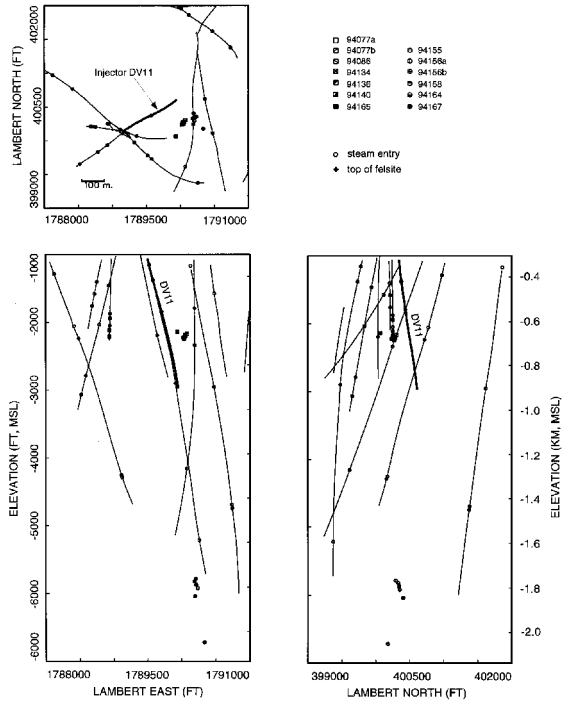

Figure 8. Relocated hypocenters for the two clusters shown in Figure 7. The arrival time picks are determined using waveform cross-correlation as described in the text.

We calculated the magnitudes of the events in the shallow cluster at M=0.3 to M=0.9, using the moment tensor inversion procedure described in a previous report (Kirkpatrick et. al., 1996), and then converting scalar moment to magnitude. According to a commonly-used rule-of thumb for estimating source dimension (e.g. Scholtz, 1990), these magnitudes correspond to source rupture dimensions of about 6 to 25 m diameter. The cluster is only 25 m across; therefore, it appears that these events are occurring in virtually the same place, perhaps even on the same rupture surface.

The deep cluster is located almost directly below the shallow cluster. The vertical dimension of the cluster (100 m, with one outlier 200 m below) as a whole is probably greater than the source dimension of the individual events, which range in magnitude from M=0.5 to M=1.0 (indicating source dimensions of 12 to 25 m diameter). The spatial distribution of the events as located may therefore be significant. The relative vertical position of the events in the cluster did not change between the routine location and the relative location, with the exception of the last event, 167, lending confidence to this assertion. (The relative location of event 098 was not determined). The deep events do not progress along the linear feature with time but rather jump up and down along the vertical trend with time.

DISCUSSION AND CONCLUSIONS

In general, injection at DV11 resulted in increased levels of seismicity. However, the increased seismicity also corresponded to increased flow rates in the production wells. It should also be noted that while there was not a lag time between injection and steam production rates, there was up to a several month lag time between injection and increased seismicity. In addition, it appears that there was a threshold of injection which caused increased seismicity, but once the system is primed, lower injection rates also increased the seismicity, i.e. as injection continued, the lag time between injection and seismicity decreased.

In terms of event attributes, it appears that event clusters are located tightly around and beneath DV11, and do not, in general, extend to production wells. However, the broader seismicity pattern defined by all of the events indicate that the events extend toward the wells with the highest production rate increases. At this point we do not have independent evidence of the location of the injected fluid, but if the earthquake locations are indicative of the fluid path, it appears that the fluid does not travel a direct route to the production well, i.e. flow is fracture and/or fault controlled. The MEQ pattern also suggests that some fluid may be lost out of the bottom of the reservoir (may be only temporarily).

The “cluster” patterns indicate that for a portion of the events they repeat locations in very small (25m) volumes. They also have linear features, indicating occurrence on single planes. Improved locations on all events may reveal much more of a linear nature to the “clouds” of events rather than the “tubes” of events. Last, but not least, the source mechanisms are mainly negative volumetric (closing) possibly indicating cooling due to injection. This is in contrast to our past work where up to 60% of events were opening types where one includes a field-wide sample. Therefore, by looking at an area dominated by injection (DV11), we are beginning to understand the mechanics of the events.

Future work will focus on including more events in the cluster analysis approach, expanding to production areas as well as injection areas defined by

the 1997 injection from Lake County. Also, different time scales and magnitude scales will be examined by investigating the correlation between rate, location, size and nature (source mechanism) of seismicity as a function of injection and production parameters.

ACKNOWLEDGMENTS

The work was supported by the Assistant Secretary for Energy Efficiency and Renewable Energy, Office of Geothermal Technologies of the US Department of Energy under contract No. DE-AC03-76SF00098. We would also like to thank Unocal Geothermal, NCPA, and Calpine for their cooperation and data.

REFERENCES

Eberhart-Phillips, D., and D. H. Oppenheimer (1984), "Induced seismicity in The Geysers geothermal area, California, J. Geophys. Res. **89**, 1191-1207.

Kirkpatrick, A., J. E. Peterson, Jr., and E. L. Majer (1995), "Microearthquake monitoring at the Southeast Geysers using a high-resolution digital array," Proc. 20th Workshop on Geotherm Res. Eng., Stanford University, 79-89.

Kirkpatrick, A., J. E. Peterson, Jr., and E. L. Majer (1996), "Source mechanisms of microearthquakes at the Southeast Geysers geothermal field, California," Proc. 21st Workshop on Geotherm Res. Eng., Stanford University, 359-366.

Kirkpatrick, A., J. E. Peterson, Jr., and E. L. Majer (1997), "Three-dimensional compressional- and shear-wave seismic velocity models for the Southeast Geysers Geothermal Field, California," Proc. 22nd Workshop on Geotherm Res. Eng., Stanford University, 399-410.

Nadeau, R. M., W. Foxall, and T. V. McEvilly (1995), "Clustering and periodic recurrence of microearthquakes on the San Andreas fault at Parkfield California," Science **267**, 503-507.

Scholtz, C. H. (1990), The Mechanics of Earthquakes and Faulting, Cambridge University Press, p. 183.

Voge, E., B. Koenig, J. L. Smith, S. Enedy, J. J. Beall, M.C Adams, and J. Haizlip (1994), "Initial findings of The Geysers Unit 18 Cooperative Injection Project," Geotherm. Resour. Counc. Trans. **18**, 353-357.